

## Filling empty states in a CuPc single layer on the Au(110) surface via electron injection

Antonio Calabrese,<sup>1,2</sup> Luca Floreano,<sup>3</sup> Alberto Verdini,<sup>3</sup> Carlo Mariani,<sup>1,2</sup> and Maria Grazia Betti<sup>1,2</sup>

<sup>1</sup>*Dipartimento di Fisica, Università di Roma La Sapienza, Piazzale Aldo Moro 5, I-00185 Roma, Italy*

<sup>2</sup>*CNISM, Dipartimento di Fisica, Università di Roma La Sapienza, I-00185 Roma, Italy*

<sup>3</sup>*CNR-INFM Laboratorio Nazionale TASC, Basovizza SS-14, Km 163.5, I-34012 Trieste, Italy*

(Received 12 January 2009; revised manuscript received 24 February 2009; published 31 March 2009)

An ordered copper-phthalocyanine (CuPc) single layer deposited on the Au(110) surface has been electron-doped by exposition to potassium. Progressive occupation of the former lowest unoccupied molecular orbitals (LUMOs) up to the filling of the twofold degenerate LUMO and LUMO+1 and LUMO+2 levels, has been detected by near-edge x-ray absorption spectroscopy spectra. The electronic states filled by electron transfer from the alkali atoms are localized at the interface, and the process induces a redistribution of the density of states with a conspicuous decrease in spectral density at the Fermi level. Localization of the final states, sudden decrease in density of states at the Fermi level, minor screening of the electron-hole excitations, and enhanced excitonic effects of doped CuPc with respect to the pristine CuPc single-layer concur to suggest that the electron injection produces a Mott insulator where correlation effects dominate the electronic properties.

DOI: [10.1103/PhysRevB.79.115446](https://doi.org/10.1103/PhysRevB.79.115446)

PACS number(s): 73.20.-r, 79.60.Jv

### I. INTRODUCTION

Design of organic nanostructures at surfaces is a topic of intense research for the advancement of nanotechnology and molecular-based devices. Engineering of these devices requires an atomic level understanding of the parameters that control the structure and function of these flexible molecular architectures. Several open questions enliven the scientific debate, primarily referred to as organic/inorganic interfaces, i.e., the strength of interaction and the charge-carrier injection control. Although organic materials have lower performance (mobility, etc.)<sup>1,2</sup> than the inorganic counterpart, a careful experimental study to gauge the electronic states and the electron and hole injection barriers at highly ordered hybrid interfaces is essential for constructing reliable models for the transport phenomena. The ability to modify the electronic properties of materials building up novel molecular architectures also via charge donation or acceptance from dopants plays a crucial role in semiconductor electronics. As devices shrink in size, the use of dopants will present new challenges since variations in dopant distribution yield large changes in device performance.<sup>3,4</sup> Experimental investigation of electron doping of  $\pi$ -conjugated systems shows a reduction in the hole injection barrier.<sup>5-11</sup>

Metal-phthalocyanines (MPcs), semiconductor in the condensed phase, can be turned metallic through alkali doping as observed by transport measurements,<sup>12,13</sup> and the electron doping appears to take place in the twofold degenerate lowest unoccupied molecular orbital (LUMO) as a function of the molecular level occupation. On the other hand, photoemission studies of MPC layer *n*-doped with alkali metals do not present any spectral density of electronic states at the Fermi level, both when the MPC molecules are arranged in thin films<sup>14,15</sup> and when they are adsorbed as few layers.<sup>11</sup> However, neither the charge donation processes nor the physical reasons of the occurrence of insulator-metal-insulator transition in the molecular film and/or at the hybrid interfaces has been yet fully clarified. The experimental results for a single-layer of CuPc (CuC<sub>32</sub>H<sub>16</sub>N<sub>8</sub>), compared

with those on CuPc thin-films, present a different response to the electron doping, albeit both systems do not present any insulator-metal transition as detected by the electronic spectral density at the Fermi level.<sup>8,11</sup>

Within this context, we electron-doped a CuPc single layer (SL), controlling the filling of the empty states by means of near-edge x-ray absorption fine-structure spectroscopy (NEXAFS), and the evolution of the filled-induced density of states by means of high-resolution photoemission. We show that the electron injection of the CuPc single layer concerns not only the LUMO state, as observed for the CuPc thin films, but also the empty states located at higher energy (LUMO+1 and LUMO+2), giving rise to a more complex redistribution of the density of the electronic states. In this work, we clarify the role of the CuPc/Au interaction at the interface and of the electron injection, and we suggest an inescapable contribution of the electron correlation for the doped MPC molecule at the interface.

### II. EXPERIMENT

Core-level photoemission and NEXAFS experiments were carried out at the Advanced Line for Overlayer, Interface and Surface Analysis (ALOISA) beamline of the Elettra synchrotron radiation facility in a ultrahigh vacuum (UHV) chamber, with base pressure better than  $1 \times 10^{-10}$  mbar. Surface quality and cleanness were checked by means of x-ray photoemission spectroscopy (XPS). XPS spectra were measured with 500 eV photon energy (overall energy resolution 180 meV) and the binding-energy (BE) scale was calibrated using the substrate metal Fermi edge. Photoelectrons were taken at normal emission with the hemispherical analyzer in constant pass energy mode (10 eV). The grazing incidence angle was fixed at  $\approx 6^\circ$  from the surface plane for all XPS spectra, enhancing the surface sensitivity. The carbon and nitrogen *K*-edge NEXAFS spectra were obtained in the partial electron yield mode by means of a channeltron with a  $-200$  V bias on the grid in order to reject secondary electrons. The photon energy, in the 280–320 eV and 395–415

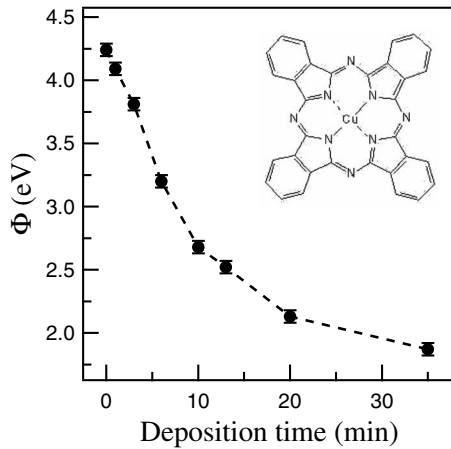


FIG. 1. Work function change at the CuPc-SL on Au(110) as a function of K deposition time. Inset: sketch of CuPc molecule.

eV energy ranges with a resolution of 100 and 120 meV for C and N 1s core levels, respectively, was selected by the ALOISA monochromator.<sup>16</sup> The NEXAFS spectra were collected with the electric field polarization ( $p$ ) parallel to the x-ray scattering plane and in grazing incidence, such as to enhance the sensitivity to the  $\pi$  states.

The Au(110)-(1 $\times$ 2) substrate surface was prepared by subsequent Ar<sup>+</sup> ion sputtering-annealing cycles (1000 eV and 720 K, followed by 500 eV and 520 K). CuPc was evaporated from boron-nitride and resistively heated quartz crucibles in UHV, and the nominal thickness was measured via an oscillating quartz thickness monitor. The CuPc molecules have been deposited on the so-prepared Au substrate with a deposition rate of less than 1 Å/min. Potassium was sublimated through a SAES-Getters dispenser, keeping the pressure in the low 10<sup>-10</sup> mbar range during deposition.

The high-resolution ultraviolet photoelectron spectroscopy (HR-UPS) spectra were collected by means of a Scienta SES-200 hemispherical analyzer in the LOTUS laboratory, at 16 meV overall energy resolution, with photoelectrons excited by a helium discharge source (He I $\alpha$  photons,  $h\nu = 21.218$  eV). They were analyzed in the emission plane integrating over  $\pm 8^\circ$ , taken at normal emission and at 20° out-of-normal emission, to enhance surface sensitivity.

The work function change was measured by the low kinetic-energy cut-off variation after negatively biasing the sample (-9 V) with respect to ground. Alkali doping of the CuPc single layer produces a strong work function ( $\Phi$ ) lowering by 2.4 eV at saturation coverage (Fig. 1), indicating a strong dipolar change, as also observed for Cs deposition on the CuPc-SL.<sup>11</sup>

### III. RESULTS AND DISCUSSION

#### A. Filling empty states: Absorption spectra

The NEXAFS spectra at the carbon and nitrogen  $K$  edges recorded from a single layer of CuPc deposited on the Au(110) surface are reported in Figs. 2(a) and 2(b), respectively. In the insets to the figures, we report the corresponding carbon 1s and nitrogen 1s core-level photoemission data

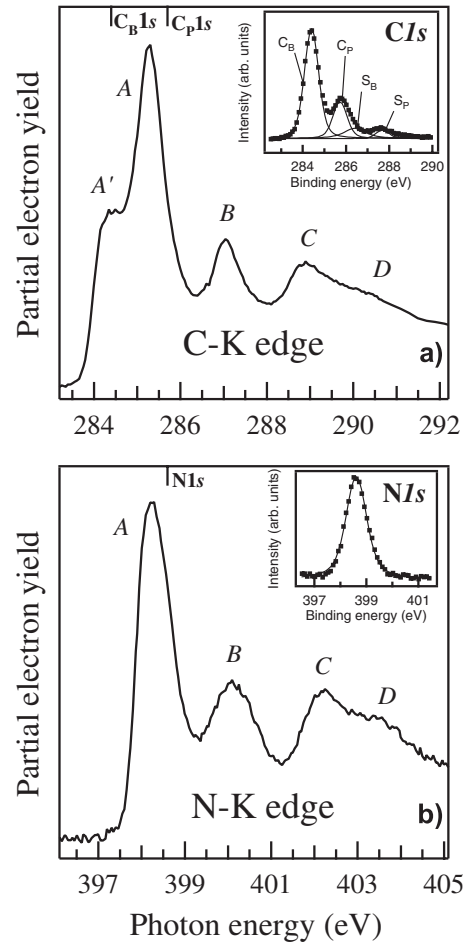


FIG. 2. NEXAFS absorption spectra from the CuPc-SL/Au(110), (a) from the carbon  $K$  edge, and (b) from the nitrogen  $K$  edge. The corresponding 1s core-level binding-energy position is marked in the top lines. In the insets, the C 1s and N 1s core-level photoemission data, along with a least-square fitting analysis, are shown.

of the CuPc-SL, together with a least square fit analysis. The C 1s core-level line shape can be deconvoluted in two main features attributed to aromatic carbon atoms in the benzene ring ( $C_B$ ) and to pyrrole carbon atoms linked to nitrogen ( $C_P$ ); there are two more peaks due to  $\pi$ - $\pi$  satellites ( $S_B$  and  $S_P$ ) referred to the  $C_B$  and  $C_P$  peaks, respectively, in agreement with the C 1s core-level line shape previously measured on CuPc thin-films.<sup>14,17-20</sup> The N 1s spectrum presents a single component although two different nitrogen sites can be identified in the molecule macrocycles. However, the N 1s fit obtained with two components (with a relative shift of about 0.3 eV) is not significantly relevant to deconvolute the contribution of the unoccupied electronic states accessed in the NEXAFS nitrogen  $K$ -edge spectra. It is worth to point out the absence of the shake-up satellite relative to the highest occupied molecular orbital (HOMO)-LUMO transition that has been observed for a CuPc thin film,<sup>15,21,22</sup> indicating an electron-hole screening exerted by the underlying metal substrate at the SL-CuPc coverage.

The main absorption features of the carbon  $K$ -edge and nitrogen  $K$ -edge NEXAFS spectra of the CuPc-SL grown on

Au(110) [Figs. 2(a) and 2(b)] are comparable to those taken for CuPc in the gas phase<sup>19</sup> and in the condensed molecular phase as thin film prepared on different substrates.<sup>20,23,24</sup> It is worth to notice the absence of a strong interaction of the CuPc macrocycles with the underlying metal surface involving the empty molecular states even if the CuPc molecules are lying on the metal Au(110) surface in a planar geometry. In fact, the highly ordered CuPc-SL on the Au(110)-(1×2) surface presents a (5×3) symmetry, as detected by the well-defined low-energy electron diffraction (LEED) pattern,<sup>25,26</sup> where the threefold reconstruction is driven by the substrate atoms rearrangement with larger missing rows, and the molecules adopt an almost flat-lying structure along the troughs of Au channels.<sup>27</sup> Large  $\pi$ -conjugated organic molecules, such as polyacenes or 3,4,9,10-perylene-tetracarboxylicdianhydride (PTCDA), often adopt a similar flat-lying geometry when deposited on metal surfaces,<sup>28,29</sup> and in these cases there are experimental evidences and theoretical predictions that bring into evidence an interaction with the underlying metal, with electron charge filling the empty molecular states, as observed in NEXAFS and photoemission studies.<sup>30–32</sup>

We concentrate our analysis in the energy region above the absorption edge, where excitations from the 1s core level to empty states of  $\pi^*$  character are probed, while we do not show the transitions to the higher-energy  $\sigma^*$  symmetry states. The assignment of the sharp absorption peaks observed in the carbon and nitrogen *K* edges can be done also taking into account previous reports on CuPc thin films.<sup>20,23,24</sup> The carbon *K* edge shows a shoulder *A'* (at 284.4 eV) close to the sharp peak *A* centered at 285.3 eV, a structure *B* located at 287.0 eV, and a broad feature with two peaks at 288.9 eV (*C*) and at 290.5 eV (*D*). The  $\pi^*$  excitations from the C 1s initial states located at carbon atoms in the pyrrole sites give origin to the main peak *A*. The first shoulder (*A'*) can be attributed to excitations into the LUMO level of  $\pi^*$  character from the C 1s level of the benzene carbon atoms as the energy shift from the main absorption peak *A* basically reflects the initial state energy splitting of the C 1s  $C_B$  and  $C_P$  peaks, as reported in the inset to Fig. 2(a). The energy shift discrepancy (0.4 eV) can be ascribed to a larger excitonic effect experienced by the transition from initial states involving the pyrrole ring, consistent with theoretical predictions stating a higher delocalization of the electron density onto carbon atoms on the benzene ring than on the C-N bonds.<sup>20</sup> Despite the intensity ratio expected by simple counting stoichiometrically the benzene and pyrrole carbon atoms, the higher intensity of peak *A* indicates that the final LUMO presents a dominant contribution from the pyrrole rings. There is a minor contribution to peak *A* from the carbon atoms of the benzene rings, but its final density of states is more delocalized resulting in broad structures.<sup>20</sup> The assignment of the features *B-D* to pyrrole and/or benzene rings is more controversial.<sup>19,20</sup> The *B* feature was assigned to excitations toward the LUMO+1 level from carbon atoms in the benzene rings, and the broad *C* band has been ascribed to transitions to the higher empty molecular states (LUMO+2), delocalized on the molecule macrocycle, but mainly located on the C-N bondings, on the basis of self-consistent field theoretical calculations.<sup>19</sup> Very recently, the *B* and *C* peaks have

been attributed to a predominant contribution from carbon atoms of the pyrrole rings.<sup>20</sup> We attribute the *B*, *C*, and *D* features to transition mainly involving the pyrrole ring, for their strong similarities in both the carbon and nitrogen *K* edges<sup>20,23,24</sup> and for the evolution of the absorption final states upon potassium deposition, as described below.

The absorption spectrum at the nitrogen *K* edge [Fig. 2(b)] exhibits four peaks (*A*, *B*, *C*, and *D*), attributed to N 1s- $\pi^*$  excitations. The energy of the nitrogen *K* edge has been aligned to that of the carbon *K* edge [Fig. 2(a)] by considering the binding energy of their respective  $C_P$  1s (carbon in the pyrrole ring) and N 1s core levels. The almost coincident energy position with respect to the edge and line shape of the *A-D* peaks of the nitrogen *K* absorption with the corresponding structures at the carbon *K* absorption suggests that the  $\pi^*$  empty states localized in the macrocycle pyrrole ring are available final states for electronic transitions from both the carbon and nitrogen atoms. The absence of peak *A'* at the nitrogen *K* edge confirms its attribution to absorption from C atoms located at the benzene rings. The slight differences of *A-D* features in the carbon and nitrogen *K* edges can be ascribed mainly to the energy distribution of the initial C and N nonequivalent 1s states. These effects suggest common  $\pi$ -symmetry molecular orbitals mainly located on the C-N bonding but with a degree of delocalization that guarantees the similar distribution of the  $\pi^*$  final states. Furthermore, taking into account the 1s core-level binding energies (C 1s component of the pyrrole ring  $C_P$  at 285.3 eV and N 1s at 398.6 eV) and the respective *K* absorption edges, we deduce comparable excitonic effects (about 0.4 eV) in the absorption process related to opening of both the C 1s and N 1s holes located on the pyrrole ring. Although the electronic charge is delocalized on the macrocycles of the phthalocyanine molecule, we can evidenciate a more localized nature of the excitations on the pyrrole ring than on the benzene ring, where the excitonic effect is negligible.

We electron-doped the CuPc-SL by exposing the molecular layer to subsequent amounts of potassium. The absorption spectra at the carbon *K* edge as a function of the K deposition time, starting from the pristine CuPc single layer up to the K saturation coverage, are shown in Fig. 3. At the very first phases of K doping, the feature *A'* suddenly decreases, indicating that the charge transfer from the K adatoms into the LUMO states is mainly located on the  $\pi^*$  states of the carbon atoms belonging to the benzene rings. Upon increasing K deposition, the absorption peak *A* starts significantly to decrease its intensity caused by the filling of the lowest unoccupied molecular orbital located with finite probability on the pyrrole carbon atoms. Furthermore, a clear attenuation of the *B* and *C* structures indicates a filling of the LUMO+1 and LUMO+2 states both involved in the process. Previous absorption spectroscopy results on the carbon *K* edge in a CuPc thin film doped with potassium shows a similar evolution of the *A* and *A'* peaks, while the *B-D* features are only slightly influenced by the electron doping.<sup>33</sup> Further K deposition do not induce any evolution of the electronic features in the NEXAFS spectra.

A progressive shift of the carbon *K*-edge NEXAFS features toward lower absorption energies (−0.4 eV) can be observed (Fig. 3), related to C atoms located on the benzene

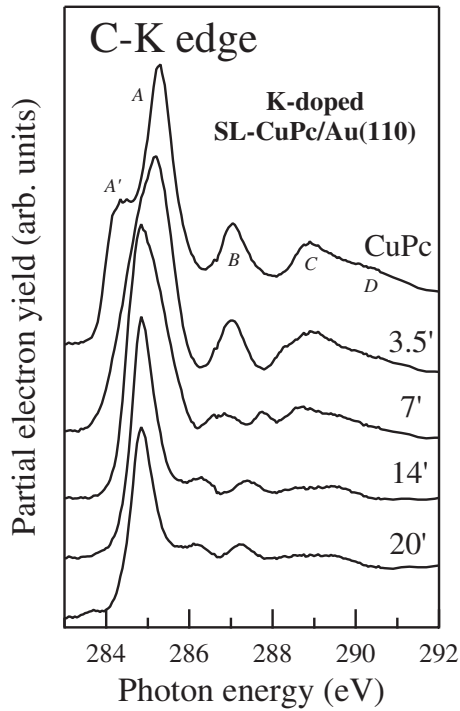


FIG. 3. Carbon *K*-edge NEXAFS absorption spectra at the K-CuPc-Au(110) interface as a function of potassium deposition time.

and pyrrole rings [see Fig. 2(a)], while the peak maximum of the C  $1s$  initial states shifts by 1.3 eV toward higher BE. As a consequence, there is an increased excitonic effect in the doped CuPc-SL (1.7 eV) and a reduction in the electron-hole screening, suggesting the hypothesis of a more localized density of final states on the C atoms in the pyrrole rings after electron injection.

The evolution of the nitrogen *K*-edge NEXAFS spectra as a function of potassium doping is depicted in Fig. 4. At the first potassium deposition, the N absorption features are basically unperturbed, except for a slight reduction in intensity of the main peak A, thus confirming that the K atoms donate charge first to the empty states localized on the benzene rings. Subsequent depositions strongly modify the distribution of the empty density of states involving LUMO, LUMO+1, and LUMO+2 levels localized on the C-N bonding, with a quenching of former *B* peak, redistribution of peaks *C-D* and emerging of a broad feature at about 407.7 eV. Such a final states modification was not observed at K-doped CuPc thin-films,<sup>33</sup> where only the first LUMO seems to be involved in the electron injection process. It is worth to notice that comparing the carbon and nitrogen NEXAFS spectra, the energy position and the line shape of the emerging features in nitrogen *K*-edge upon doping do not reproduce the evolution observed for the empty states in the carbon *K*-edge spectra. While the carbon and nitrogen *K*-edge absorption spectra of the pristine CuPc-SL look very similar [Fig. 2], upon the electron donation of K adatoms to the  $\pi^*$  empty states, the final states for electronic transitions appear clearly different for carbon and nitrogen *K* edges in the doped system. All these consequences of the K adsorption contribute to a picture of the K electron donation pro-

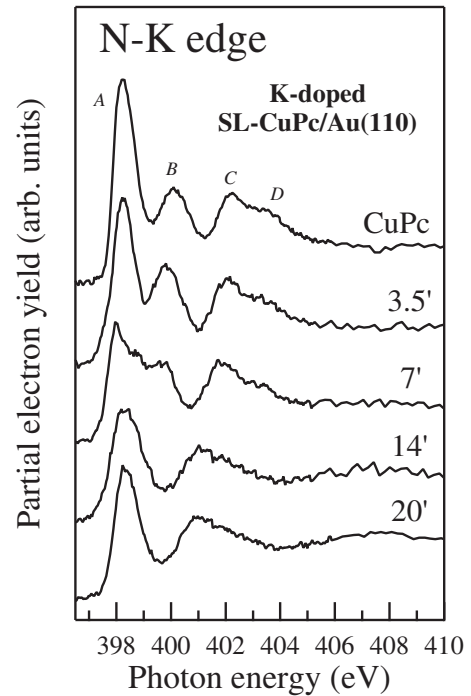


FIG. 4. Nitrogen *K*-edge NEXAFS absorption spectra at the K-CuPc-Au(110) interface as a function of potassium deposition time.

cess which results in an electron density of final states more localized in the macrocycles in the doped system with respect to the CuPc-SL.

Only for low potassium dose, the present data on the nitrogen and carbon *K*-edge line-shape evolution show similar behavior with the results of K-doped CuPc thin-film,<sup>33</sup> while high K dose causes major changes in the CuPc-SL NEXAFS spectra, particularly for the nitrogen *K*-edge. The electron doping of the CuPc-SL, namely, gives rise to a more complex stoichiometry of the potassium adsorption, involving more potassium atoms per molecule, with respect to the CuPc thin-film evolution.<sup>33</sup> More insights can be obtained by means of photoemission core-level spectroscopy: the N  $1s$ , C  $1s$ , and K  $2p$  core-level photoemission spectra of the CuPc-SL on Au(110) and after subsequent K doping are shown in Fig. 5 (N) and Fig. 6 (C and K). The centroid of the N  $1s$  core level shows an initial energy shift to higher BE at low K dose, while at higher dose it apparently reverses the energy shift. This line-shape behavior is actually due to the appearance of an additional component at lower BE, whose intensity increases upon K deposition, while the first component (associated to the pristine CuPc-SL) reduces its intensity. At saturation coverage, the lower BE-component remains as the dominant contribution to the N  $1s$  core level with a final energy shift by about  $-0.4$  eV with respect to the clean CuPc-SL feature caused by the charge transfer from the potassium to the nitrogen atoms. Furthermore, concomitant with the presence of the second core-level component, shake-up satellite peaks emerge in the high BE (low kinetic energy) side, confirmation of a reduced screening. Analogous line-shape evolution of the N  $1s$  core level has been detected by K doping a CuPc thin-film<sup>15</sup> although in that case the



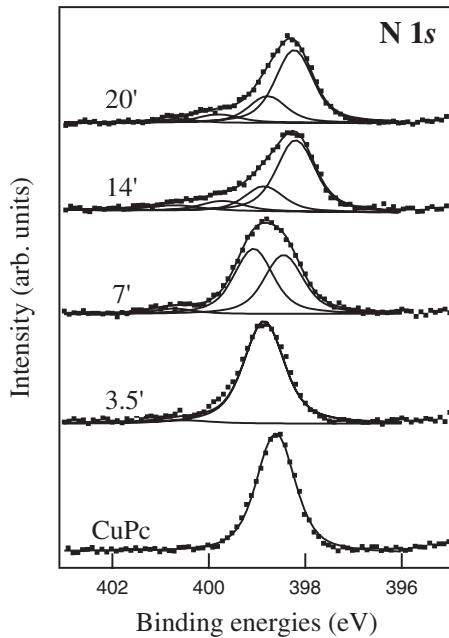


FIG. 5. XPS data from at the K-CuPc-Au(110) interface as a function of potassium deposition time: N 1s core-level evolution (dotted lines), least-square fitting analysis with single components, and their sum (continuous lines).

lower BE component does not dominate at saturation coverage. The C 1s core level presents a much more complex behavior upon doping: it is affected by a continuous broadening involving both the pyrrole ( $C_p$ ) and the benzene ( $C_B$ ) components. An unambiguous assignment of the BE shift to the specific C atoms belonging to the benzene and pyrrole

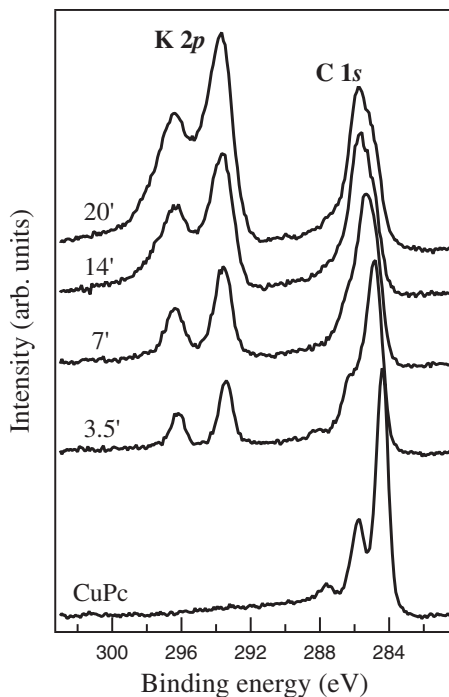


FIG. 6. K 2p and C 1s core-level evolution at the K-CuPc-Au(110) interface as a function of potassium deposition time.

ring is arduous, but the spectral evolution definitely suggests the interaction with potassium atoms in different sites of the macrocycle, with an overall peak energy shift by +1.3 eV toward higher BE. The K 2p core levels present a single component at the first doping stage, while a broadening emerges at higher K dose that can be taken into account by considering a higher binding-energy component. On the contrary, the K 2p and 3p core levels in K-doped CuPc thin film present a single structure,<sup>15</sup> indication of equivalent adsorption sites and electron charge transfer to the former LUMO. In the K-doped CuPc-SL, the first doublet is associated to K adatoms interacting with the benzene ring in the very first phases of adsorption, while the second component is caused by further K atoms interacting with the pyrrole macrocycle. Finally, the K atoms do not interact with the underlying Au substrate, as deduced by the unperturbed Au 4f core levels (not shown here). At higher K dose, the emerging of further core-level components associated to different adsorption sites cannot be excluded although a fit would have a high degree of arbitrariness. On the basis of core-level intensity evolution and of simple atomic cross section excitation calculations,<sup>34</sup> we can estimate as about 8 the number of potassium atoms interacting with each molecule. We may consider the eight K atoms as the doping actors, while we cannot exclude that a small percentage of further K atoms adsorb with less interaction with the system. Further exposition to K produces light traces of contaminants, inducing a small increase in the K 2p core-level intensity that we disregarded.

The estimation from the core-level analysis confirms the picture of K interaction with the molecular macrocycles in two phases, as depicted in the NEXAFS data evolution: we can hypothesize that the potassium adatoms contribute in different adsorption sites first involving the benzene sites than the pyrrole rings with minor screening effects associated to a more localized density of states.

## B. Filled states: Photoemission results

The normal-emission photoemission data from the valence band of the CuPc-SL deposited on the Au(110) surface as a function of K deposition is depicted in Fig. 7. After the deposition of a single layer of CuPc, the surface states, attributed to the  $(1 \times 2)$  reconstructed Au(110) surface, suddenly disappear and new electronic features emerge, mainly attributed to the Au surface reconstruction ( $\times 3$  symmetry)<sup>25,26</sup> due to the widening of the Au channels. The evolution of the electron spectral density in the energy region close to the Fermi level ( $E_F$ ) is presented in Fig. 8. The data were collected with incidence photons at  $20^\circ$  out-of-normal emission to enhance sensitivity to the surface and to the  $\pi$ -symmetry molecular states at the interface. The peak at 1.24 eV BE has a clear molecular origin and it is attributed to the HOMO. It lies slightly shifted to lower BE with respect to the HOMO measured in the CuPc thin film.<sup>11</sup> At the first potassium deposition, the HOMO-related structure remains almost unperturbed, and a potassium induced feature appears close to the Fermi level. At subsequent K dose ( $3'$ ), the HOMO peak decreases its intensity eventually disappearing

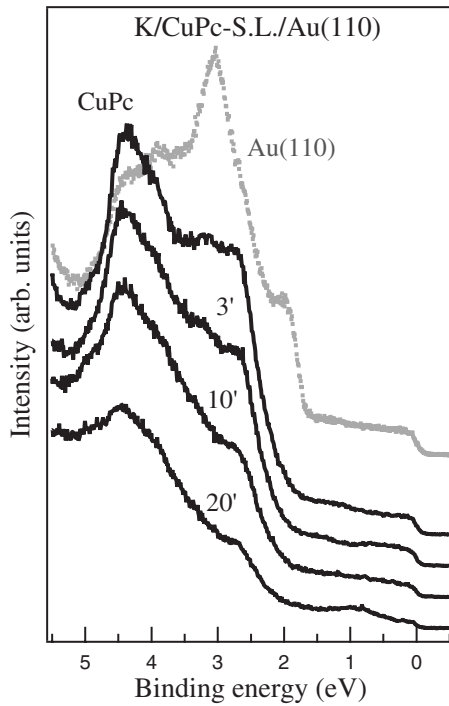


FIG. 7. HR-UPS normal-emission data from the valence band region of the K-CuPc-Au(110) as a function of potassium deposition time. The spectrum of clean Au(110) is shown for comparison.

(6') in the redistributed spectral density. Furthermore, the slight feature close to  $E_F$  shifts to higher BE and increases its intensity, indicating the occupation of the first former LUMO state, as recently observed for analogous system (Cs-doping of a CuPc-SL).<sup>11</sup> A second structure emerges below  $E_F$  and becomes clearly visible at 13' of K deposition time. Thus, after the occupation of the first former-LUMO, subsequent former-empty states are filled up to K saturation coverage. The progressive occupation of the LUMO states and the appearance of a second structure in the spectral density is accompanied by a continuous reduction in the spectral density at  $E_F$ , achieving an almost insulating phase at saturation K coverage. This evidence is contributory to the presumption of the rise of electron correlation effects in the evolution of the absorption spectra. In a recent paper,<sup>11</sup> we hypothesized that the introduction of electronic charge in the CuPc-SL activates the Coulomb repulsion between electrons trapped in the former-LUMO states. The ongoing debate on the origin and the evolution of the electronic spectral density hypothesizes both a contribution from the redistribution of the density of states due to CuPc interaction with the Au(110) surface and the contribution of further molecular empty states in the electron injection process. The combined photoemission and absorption results presented here make clear

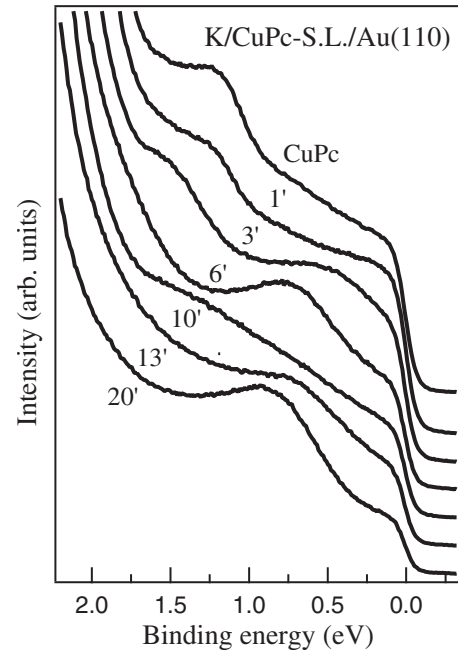


FIG. 8. HR-UPS data taken at 20° out-of-normal emission of the K-CuPc-Au(110) as a function of potassium deposition time.

this point, attributing the presence of two main contributions to the electronic spectral density to the occupation of LUMO and LUMO+1,2 states and confirm and reinforce the hypothesis of a Mott insulator, where correlation effects due to localized states results in a repulsion energy  $U$  larger than the single-particle bandwidth.

#### IV. CONCLUSIONS

Electron injection through potassium doping of a CuPc single layer on Au(110) produces major changes in the absorption spectra of the carbon and nitrogen  $K$  edges, in their respective  $1s$  core levels and in the electronic spectral density close to the Fermi level. These important changes involve subsequent occupation of former unoccupied molecular states, with the K atoms associated to different adsorption sites, first close to the benzene rings then to the pyrrole rings. The filling of the empty LUMO states induces more localized states, a decreased screening effect at the interface and a lowering of the density of states at the Fermi level. These experimental evidences suggest a general picture where electron correlation effects associated to the localization play a major role.

#### ACKNOWLEDGMENTS

We are grateful to Aloisa beamline staff and to F. Crispoldi for the experimental support. Work granted by funds of the Università di Roma La Sapienza.

- <sup>1</sup>N. Karl, *Organic Nanostructures: Science and Applications* (IOSS Amsterdam, 2002).
- <sup>2</sup>A. Kahn, N. Koch, and W. Gao, *J. Polym. Sci., Part B: Polym. Phys.* **41**, 2529 (2003).
- <sup>3</sup>P. A. Packan, *Science* **285**, 2079 (1999).
- <sup>4</sup>S. R. Schofield, N. J. Curson, M. Y. Simmons, F. J. Rueß, T. Hallam, L. Oberbeck, and R. G. Clark, *Phys. Rev. Lett.* **91**, 136104 (2003).
- <sup>5</sup>T. Minakata, I. Nagoya, and M. Ozaki, *J. Appl. Phys.* **69**, 7354 (1991).
- <sup>6</sup>T. Minakata, M. Ozaki, and H. Imai, *J. Appl. Phys.* **74**, 1079 (1993).
- <sup>7</sup>W. Gao and A. Kahn, *J. Phys.: Condens. Matter* **15**, S2757 (2003).
- <sup>8</sup>Y. Gao and L. Yan, *Chem. Phys. Lett.* **380**, 451 (2003).
- <sup>9</sup>B. Fang, H. Zhou, and I. Homna, *Appl. Phys. Lett.* **86**, 1 (2005).
- <sup>10</sup>L. Giovanelli, P. Vilmercati, C. Castellarin-Cudia, J.-M. Thémelin, L. Porte, and A. Goldoni, *J. Chem. Phys.* **126**, 044709 (2007).
- <sup>11</sup>M. G. Betti, F. Crispoldi, A. Ruocco, and C. Mariani, *Phys. Rev. B* **76**, 125407 (2007).
- <sup>12</sup>M. Craciun, S. Rogge, and A. Morpurgo, *J. Am. Chem. Soc.* **127**, 12210 (2005).
- <sup>13</sup>M. Craciun, S. Rogge, M.-J. den Boer, S. Margadonna, K. Prasad, Y. Iwasa, and A. Morpurgo, *Adv. Mater. (Weinheim, Ger.)* **18**, 320 (2006).
- <sup>14</sup>T. Schwieger, H. Peisert, M. S. Golden, M. Knupfer, and J. Fink, *Phys. Rev. B* **66**, 155207 (2002).
- <sup>15</sup>O. Molodtsova, V. Zhilin, D. Vyalikh, V. Aristov, and M. Knupfer, *J. Appl. Phys.* **98**, 093702 (2005).
- <sup>16</sup>R. Gotter, A. Ruocco, A. Morgante, D. Cvetko, L. Floreano, F. Tommasini, and G. Stefani, *Nucl. Instrum. Methods Phys. Res. A* **467-468**, 1468 (2001).
- <sup>17</sup>G. Dufour, C. Poncey, F. Rochet, H. Roulet, M. Sacchi, M. D. Santis, and M. D. Crescenzi, *Surf. Sci.* **319**, 251 (1994).
- <sup>18</sup>M. K. H. Peisert and J. Fink, *Surf. Sci.* **515**, 491 (2002).
- <sup>19</sup>F. Evangelista, V. Carravetta, G. Stefani, B. Jansik, M. Alagia, S. Stranges, and A. Ruocco, *J. Chem. Phys.* **126**, 124709 (2007).
- <sup>20</sup>O. V. Molodtsova, M. Knupfer, V. V. Maslyuk, D. V. Vyalikh, V. M. Zhilin, Y. A. Ossipyan, T. Bredow, I. Mertig, and V. Y. Aristov, *J. Chem. Phys.* **129**, 154705 (2008).
- <sup>21</sup>H. Peisert, M. Knupfer, T. Schwieger, J. M. Auerhammer, M. S. Golden, and J. Fink, *J. Appl. Phys.* **91**, 4872 (2002).
- <sup>22</sup>V. Y. Aristov, O. V. Molodtsova, V. M. Zhilin, D. V. Vyalikh, and M. Knupfer, *Phys. Rev. B* **72**, 165318 (2005).
- <sup>23</sup>V. Y. Aristov, O. V. Molodtsova, V. Maslyuk, D. Vyalikh, V. Zhilin, Y. Ossipyan, T. Bredow, I. Mertig, and M. Knupfer, *Appl. Surf. Sci.* **254**, 20 (2007).
- <sup>24</sup>V. Y. Aristov, O. V. Molodtsova, V. V. Maslyuk, D. V. Vyalikh, V. M. Zhilin, Y. A. Ossipyan, T. Bredow, I. Mertig, and M. Knupfer, *J. Chem. Phys.* **128**, 034703 (2008).
- <sup>25</sup>F. Evangelista, A. Ruocco, V. Corradini, C. Mariani, and M. G. Betti, *Surf. Sci.* **531**, 123 (2003).
- <sup>26</sup>F. Evangelista, A. Ruocco, D. Pasca, C. Baldacchini, M. G. Betti, V. Corradini, and C. Mariani, *Surf. Sci.* **566-568**, 79 (2004).
- <sup>27</sup>L. Floreano, A. Cossaro, R. Gotter, A. Verdini, G. Bavdek, F. Evangelista, A. Ruocco, A. Morgante, and D. Cvetko, *J. Phys. Chem. C* **112**, 10794 (2008).
- <sup>28</sup>C. Baldacchini, C. Mariani, and M. G. Betti, *J. Chem. Phys.* **124**, 154702 (2006).
- <sup>29</sup>Y. Zou, L. Kilian, A. Schöll, T. Schmidt, R. Fink, and E. Umbach, *Surf. Sci.* **600**, 1240 (2006).
- <sup>30</sup>M. G. Betti, A. Kanjilal, and C. Mariani, *J. Phys. Chem. A* **111**, 12454 (2007).
- <sup>31</sup>A. Ferretti, C. Baldacchini, A. Calzolari, R. DiFelice, A. Ruini, E. Molinari, and M. G. Betti, *Phys. Rev. Lett.* **99**, 046802 (2007).
- <sup>32</sup>N. Koch *et al.*, *J. Am. Chem. Soc.* **130**, 7300 (2008).
- <sup>33</sup>O. V. Molodtsova, M. Knupfer, V. Y. Aristov, D. V. Vyalikh, V. M. Zhilin, and Y. A. Ossipyan, *J. Appl. Phys.* **103**, 053711 (2008).
- <sup>34</sup>J.-J. Yeh and I. Lindau, *At. Data Nucl. Data Tables* **32**, 1 (1985).